

无机化学学报

2017年

第33卷

第10期

目 次

综 述

基于N,C螯合 π 共轭骨架的四配位有机硼化合物及其光电应用

..... 秦妍妍 许文娟 胡长永 刘淑娟 赵 强(1705)

论 文

一种用于活细胞中检测Zn²⁺的萘酚席夫碱类荧光探针(英文)

..... 陈 邦 王少静 宋战科 郭 媛(1722)

AgI/h-MoO₃异质结的构筑及其模拟燃油光催化氧化脱硫活性

..... 甄延忠 王 杰 付梦溪 张应铮 付 峰(1731)

CaWO₄:xEu³⁺,ySm³⁺,zLi⁺红色荧光粉的制备及光学性能..... 王林香(1741)

不同锌铝比水滑石的合成及其吸附脱除水中邻苯二甲酸性能

..... 杨盈利 闫新龙 胡晓燕 周 敏(1748)

Zn₂GeO₄纳米棒的制备及发光性质..... 杨 扬 丛 妍 朱子茂

..... 过 诚 张 填 王子文 张家骅(1757)

锂离子电池 Si@void@C复合材料的制备及其电化学性能

..... 蔡建信 李志鹏 李 巍 赵鹏飞 杨震宇 吕 霽(1763)

溶剂热法制备立方状ITO粉体及其电性能..... 彭 祥 陈玉洁 刘家祥(1769)

包覆ZrO₂锂离子筛的制备及其在盐湖卤水中的吸附性能

..... 王 豪 杨喜云 尹周澜 曹改芳 徐 累(1775)

Ag₃PO₄/MoS₂纳米片复合催化剂制备及可见光催化性能

..... 阎 鑑 惠小艳 高 强 余高杰 莫云城 叶梓萌 李俊春 马梓译 孙国栋(1782)

不同水热条件下TiO₂/电气石复合材料的光催化机制..... 亓淑艳 吴 超 王德朋 胡焕岩(1789)

钛合金表面铁氧化物膜层类Fenton催化剂制备及降解苯酚性能

..... 姚忠平 陈昌举 王建康 夏琦兴 李春香 姜兆华(1797)

高分散在氮掺杂碳纳米管表面铂纳米粒子的高效甲醇电氧化性能

..... 刘晨霞 蔡跃进 王 钰 范 豪

..... 陈 强 吴 强 杨立军 王喜章 胡 征(1805)

6-甲氧羰基-4,4'-二甲基-2,2'-联吡啶单核铜(I)双膦发光配合物(英文)

..... 曾雪花 罗燕生 何丽华 陈景林 张梦丽 廖金生 刘遂军 温和瑞(1810)

基于柔性四羧酸配体构筑的两个镉(II)配位聚合物的晶体结构及荧光性质(英文)

..... 刘 露 许春莺 李 英 王吉超 张裕平 王键吉(1817)

K₂FeO₄的合成及对含苯酚水溶液中重金属离子的去除性能(英文)

..... 何登良 刘树信 秦海利 沈 芳 王学利 刘 岚 阮期平(1825)

- 钯纳米粒子的形貌可控合成与催化性能(英文)
.....茹婷婷 初学峰 石莹岩 郑文琦 郭 研 杨小天 蒋 镛(1835)
- 基于 *N*-3-吡啶磺酰化氨基乙酸配体的 Co(II)配位聚合物的合成、晶体结构和磁性分析(英文)
.....廖蓓玲 杨鸽鸽 李石雄 蒋毅民 银秀菊(1843)
- 基于 3-乙基-2-乙酰吡嗪缩肽基甲酸甲酯的铜和锌配合物的晶体结构及荧光性质(英文)
.....毛盼东 陈泽华 王 媛 秦 莉 吴伟娜 王 元(1849)
- 基于 PbI₂ 的有机-无机杂化化合物的合成和晶体结构(英文)
.....袁国军 刘光祥 时 超 邵冬生(1855)
- 两个含二齿席夫碱配体单核镍(II)和铜(II)配合物的合成、结构及抗菌活性(英文)
.....刘 超 李沙沙 杨 敏 毕 蓉 于清泉 张 莉(1861)
- 联苯-2,4,4',6-四甲酸银、咪唑-菲啰啉-苯氧乙酸镉配位聚合物的合成、结构及与 DNA 的
相互作用(英文).....鲁 雅 吕天喜 胡未极 吴小勇 赵国良(1869)
- N*-(2-吡咯甲基)-1-苯基乙亚胺·二甲基铝的合成、结构及其催化丙交酯的活性(英文)
.....贾 斌 郝俊生 童红波 魏学红 周梅素 刘滇生(1876)
- Al 含量对 AB₅ 型储氢合金电极低温和高倍率性能的影响(英文)
.....汤争耀 周万海 朱 丁 吴朝玲 黄利武 刘 昆 陈云贵(1881)
- 基于柔性三齿配体的镉(II)和锌(II)配合物的合成、结构和荧光性质(英文)
.....吴 琪 苏 志 王红艳 董益利 胡炯圣
刘冬菊 吴 翳 徐 芸 应 翩 方 敏 刘红科(1889)
- 《无机化学学报》投稿须知(NOTICE TO AUTHORS).....(1896)

CHINESE JOURNAL OF INORGANIC CHEMISTRY

Vol.33

No.10

Oct. 2017

CONTENTS

Cover



Four-Coordinated Organoboron Compounds with π -Conjugated N,C-Chelate Ligand and Their Optoelectronic Applications

QIN Yan-Yan, XU Wen-Juan, HU Chang-Yong, LIU Shu-Juan, ZHAO Qiang

DOI:10.11862/CJIC.2017.223

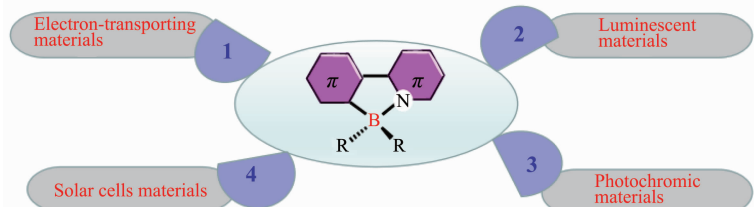
Chinese J. Inorg. Chem., **2017**,**33**:1705-1721

Reviews

Four-Coordinated Organoboron Compounds with π -Conjugated N,C-Chelate Ligand and Their Optoelectronic Applications

QIN Yan-Yan, XU Wen-Juan,
HU Chang-Yong, LIU Shu-Juan, ZHAO Qiang

DOI:10.11862/CJIC.2017.223
Chinese J. Inorg. Chem., **2017**,**33**:1705-1721

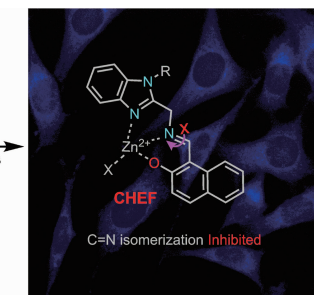


In this review, we have summarized the recent research progress on the synthesis and the applications of N,C-chelate four-coordinated organoboron compounds. These materials with strong intramolecular electron delocalization and rigid π -conjugated skeletons, are promising candidates as novel optoelectronic materials for applications in organic light-emitting diodes (OLEDs), organic field-effect transistors (OFETs), organic solar cells and sensors.

Articles

Naphthol-Based Schiff Base as a Selective Fluorescent Probe for Detecting Zn^{2+} in Living Cells (English)

CHEN Bang, WANG Shao-Jing,
SONG Zhan-Ke, GUO Yuan



DOI:10.11862/CJIC.2017.227
Chinese J. Inorg. Chem., **2017**,**33**:1722-1730

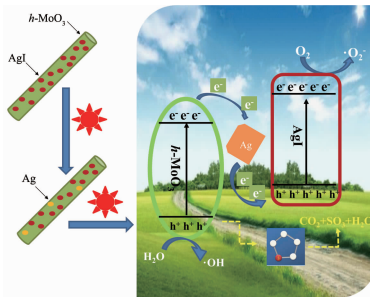
Two fluorescent probes BMO and NBMO were developed for the highly selective detection of Zn^{2+} based on C=N isomerization and chelation-enhanced fluorescence (CHEF) mechanism. The cell images showed that NBMO could be used to detect intracellular Zn^{2+} .

**AgI/h-MoO₃ Heterojunctions:
Fabrication and Photocatalytic
Oxidative Desulfurization Activity of
Simulation Fuel**

ZHEN Yan-Zhong, WANG Jie, FU Meng-Xi,
ZHANG Ying-Zheng, FU Feng

DOI:10.11862/CJIC.2017.236

Chinese J. Inorg. Chem., **2017**, *33*:1731-1740



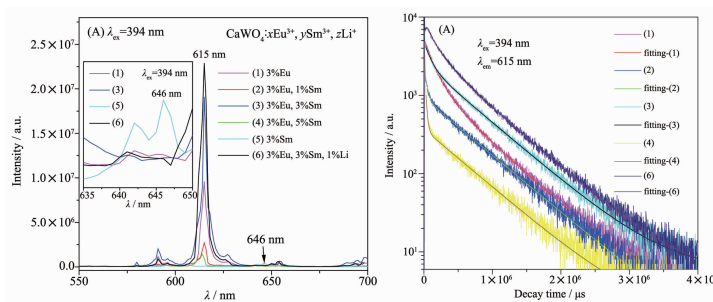
The structure AgI/h-MoO₃ transferred to Z-scheme heterojunction AgI/Ag/h-MoO₃ due to resulting in a small amount of metallic Ag in the initial stage of the photocatalytic reaction, which is favor of accelerating photoinduced electrons transfer, and enhancing separation of photoinduced electron-hole pairs contributed to the improvement of photocatalytic oxidative desulfurization activity for thiophene.

**Preparation and Luminescence
Properties of CaWO₄:*x*Eu³⁺, *y*Sm³⁺,
zLi⁺ Red Phosphors**

WANG Lin-Xiang

DOI:10.11862/CJIC.2017.213

Chinese J. Inorg. Chem., **2017**, *33*:1741-1747

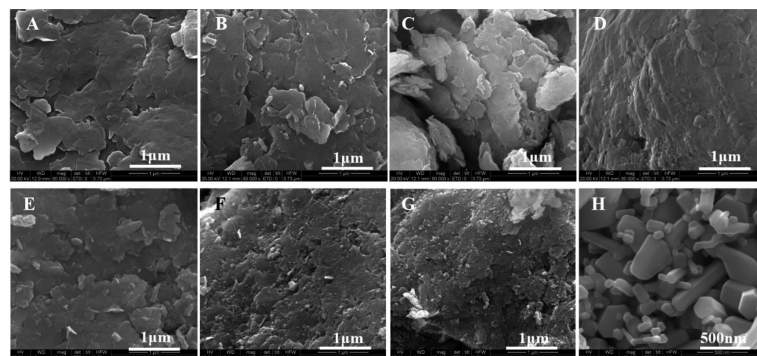


Zn/Al Hydrotalcite with Different *n*_{Zn}/*n*_{Al} Molar Ratios: Synthesis and Phthalic Acid Adsorption Behaviour

YANG Ying-Li, YAN Xin-Long,
HU Xiao-Yan, ZHOU Min

DOI:10.11862/CJIC.2017.232

Chinese J. Inorg. Chem., **2017**, *33*:1748-1756

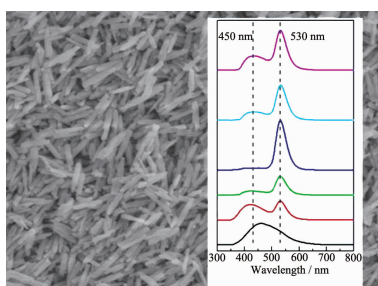


Synthesis and Luminescence Properties of Zn₂GeO₄ Nanorods

YANG Yang, CONG Yan, ZHU Zi-Mao,
GUO Cheng, ZHANG Zhen, WANG Zi-Wen,
ZHANG Jia-Hua

DOI:10.11862/CJIC.2017.235

Chinese J. Inorg. Chem., **2017**, *33*:1757-1762



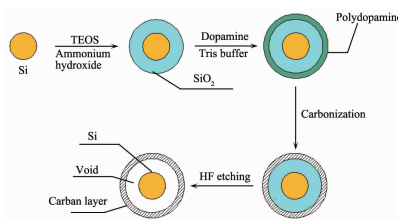
Blue-green emission-tunable Zn₂GeO₄ nanophosphor was obtained, and the PL peaks located at 350 nm and 530 nm is depended on the size of nanorods.

Synthesis and Electrochemical Performance of Si@void@C Composite Anode Material for Lithium Ion Battery

CAI Jian-Xin, LI Zhi-Peng, LI Wei,
ZHAO Peng-Fei, YANG Zhen-Yu, YU Ji

DOI:10.11862/CJIC.2017.226

Chinese J. Inorg. Chem., **2017**, *33*:1763-1768

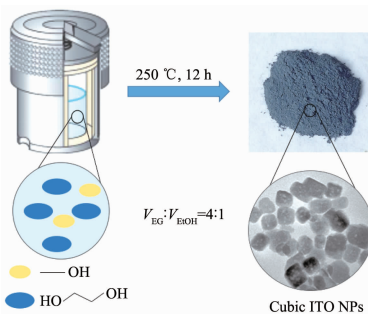


Solvothermal Synthesis and Electrical Performance of Cubic ITO Powders

PENG Xiang, CHEN Yu-Jie, LIU Jia-Xiang

DOI:10.11862/CJIC.2017.224

Chinese J. Inorg. Chem., **2017**,**33**:1769-1774



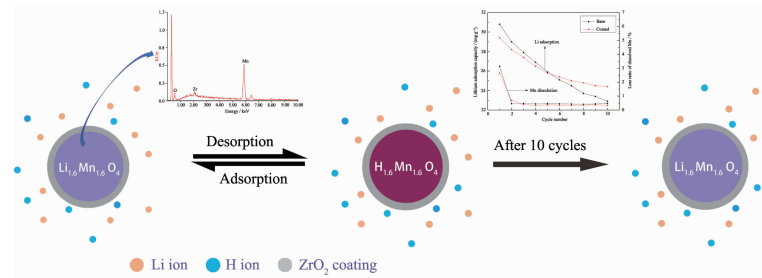
Small-sized and well-dispersed cubic shape ITO powders were synthesized using ethylene glycol and ethanol as mixed solvents. The results show the average particle size is 10.7 nm, the electric conductivity of the powder gets up to the maximum of $46.75 \text{ mS} \cdot \text{cm}^{-1}$, when the volume ratio of ethylene glycol to ethanol is 4:1.

Synthesis and Adsorption Properties of ZrO_2 -Coated Lithium Ion-Sieve from Salt Lake Brine

WANG Hao, YANG Xi-Yun, YIN Zhou-Lan, CAO Gai-Fang, XU Hui

DOI:10.11862/CJIC.2017.217

Chinese J. Inorg. Chem., **2017**,**33**:1775-1781

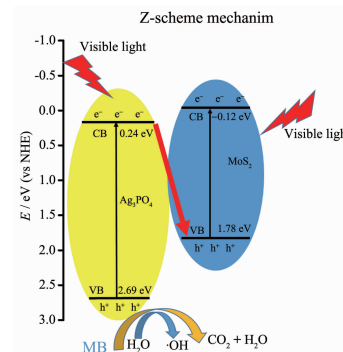


Synthesis and Visible Light Photocatalytic Performance of $\text{Ag}_3\text{PO}_4/\text{MoS}_2$ Nanosheets Composite Photocatalyst

YAN Xin, HUI Xiao-Yan, GAO Qiang, YU Gao-Jie, MO Yun-Cheng, YE Zi-Meng, LI Jun-Chun, MA Zi-Yi, SUN Guo-Dong

DOI:10.11862/CJIC.2017.212

Chinese J. Inorg. Chem., **2017**,**33**:1782-1788

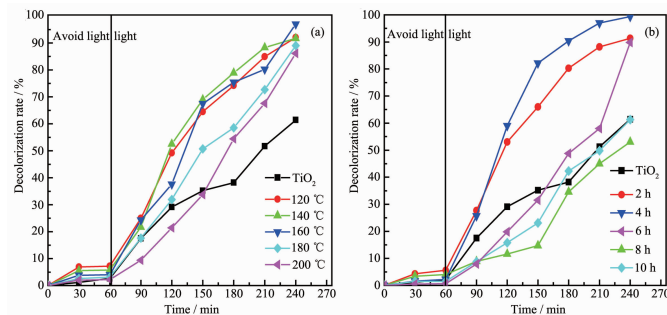


Photocatalytic Mechanism of TiO_2 /schorl Composite by Different Hydrothermal Conditions

QI Shu-Yan, WU Chao, WANG De-Peng, XU Huan-Yan

DOI:10.11862/CJIC.2017.219

Chinese J. Inorg. Chem., **2017**,**33**:1789-1796

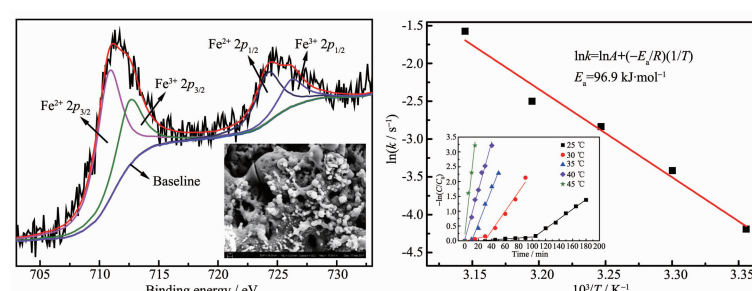


Iron Oxide Coating Fenton-like Catalysts: Preparation and Degradation of Phenol

YAO Zhong-Ping, CHEN Chang-Ju, WANG Jian-Kang, XIA Qi-Xing, LI Chun-Xiang, JIANG Zhao-Hua

DOI:10.11862/CJIC.2017.197

Chinese J. Inorg. Chem., **2017**,**33**:1797-1804

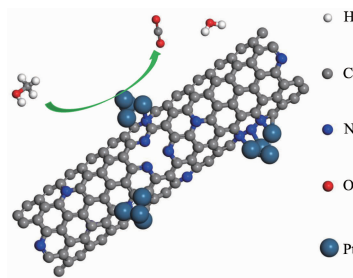


High-Efficiency Pt Catalyst Supported on Nitrogen-Doped Carbon Nanotubes for Methanol Electrooxidation

LIU Chen-Xia, CAI Yue-Jin, WANG Yu,
FAN Hao, CHEN Qiang, WU Qiang,
YANG Li-Jun, WANG Xi-Zhang, HU Zheng

DOI:10.11862/CJIC.2017.205

Chinese J. Inorg. Chem., 2017, 33:1805-1809



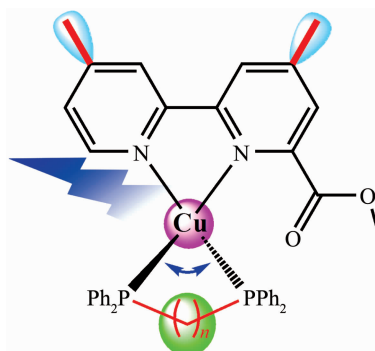
High-dispersive Pt catalysts for methanol electrooxidation were conveniently constructed owing to the nitrogen participation, and their performances evolutions are well-correlated with the controllable sizes distributions.

Luminescent Mononuclear Copper(I) Diphosphine Complexes with 6-Methoxycarbonyl-4,4'-dimethyl-2,2'-bipyridine (English)

ZENG Xue-Hua, LUO Yan-Sheng, HE Li-Hua,
CHEN Jing-Lin, ZHANG Meng-Li,
LIAO Jin-Sheng, LIU Sui-Jun, WEN He-Rui

DOI:10.11862/CJIC.2017.234

Chinese J. Inorg. Chem., 2017, 33:1810-1816



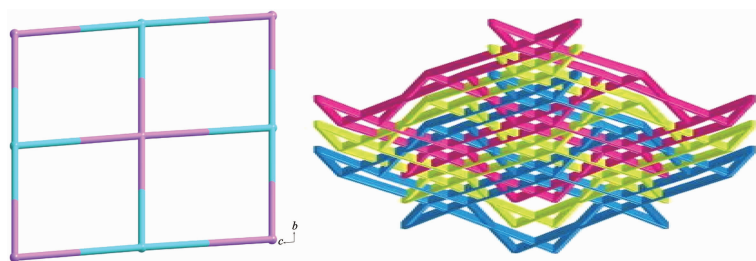
The emission properties of Cu(I) complexes are more markedly influenced by the P-Cu-P angle than the methylene chain length of diphosphine, and the introduction of two methyl substituents into the 2,2'-bipyridyl ring is effective for improving luminescence properties.

Two Cd(II) Coordination Polymers Based on Flexible Tetracarboxylic Acid Ligands: Crystal Structures and Fluorescent Properties (English)

LIU Lu, XU Chun-Ying, LI Ying,
WANG Ji-Chao, ZHANG Yu-Ping,
WANG Jian-Ji

DOI:10.11862/CJIC.2017.233

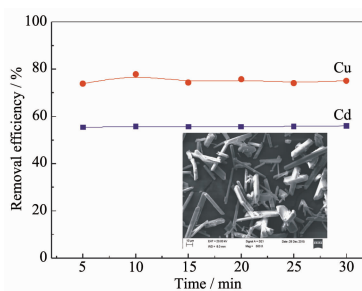
Chinese J. Inorg. Chem., 2017, 33:1817-1824



Complex **1** features a (4,4)-connected *sql* topology net with point symbol of $\{4^4 \cdot 6^2\}_2$. Complex **2** presents a trinodal (4,4,4)-connected 3D 3-fold interpenetrating *bbf* network with a Schläfli symbol of $(6^6)(6^4 \cdot 8^2)$. **1** and **2** present better thermal stabilities and different photoluminescence behaviors in the solid state.

Synthesis of K₂FeO₄ for Removing Heavy Metals in the Phenol-Aqueous Solution (English)

HE Deng-Liang, LIU Shu-Xin, QIN Hai-Li,
SHEN Fang, WANG Xue-Li, LIU Lan,
RUAN Qi-Ping



K₂FeO₄ crystals were synthesized by secondary recrystallized purification with calcium hypochlorite and iron nitrate nonahydrate as raw material. And it was used to remove Cu(II) and Cd(II) ions from phenol-aqueous solution.

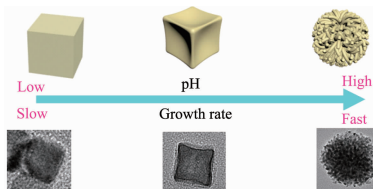
DOI:10.11862/CJIC.2017.237

Chinese J. Inorg. Chem., 2017, 33:1825-1834

Shape-Controlled Synthesis of Pd Nanocrystals with Remarkable Enhanced Catalytic Performance (English)

RU Ting-Ting, CHU Xue-Feng, SHI Ying-Yan, ZHENG Wen-Qi, GUO Yan, YANG Xiao-Tian, JIANG Kai

DOI:10.11862/CJIC.2017.193
Chinese J. Inorg. Chem., 2017, 33:1835-1842

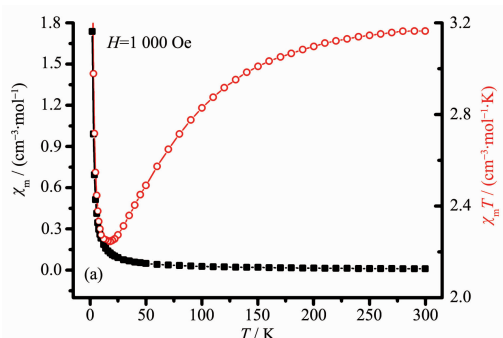


A morphology evolution of Pd nanocrystals has been induced by using OTAB-Na as the capping agent. In the following catalytic test of liquid-phase reduction of 4-NP by AB, the dendritic nanosphere is more active than concave cube, indicating a typical shape-dependent catalytic properties.

Syntheses, Structures and Magnetic Analysis of Co(II) Coordination Polymer Based on *N*-(Pyridine-3-sulfonyl amino) Acetate (English)

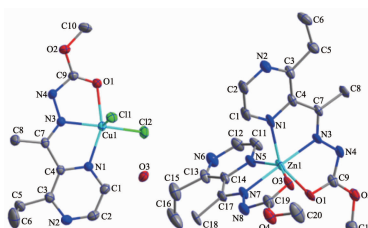
LIAO Bei-Ling, YANG Ge-Ge, LI Shi-Xiong, JIANG Yi-Min, YIN Xiu-Ju

DOI:10.11862/CJIC.2017.189
Chinese J. Inorg. Chem., 2017, 33:1843-1848



Cu(II) and Zn(II) Complexes Based on Methyl (1-(3-Ethylpyrazin-2-yl) ethylidene)carbazate: Crystal Structures and Fluorescence Properties (English)

MAO Pan-Dong, CHEN Ze-Hua, WANG Yuan, QIN Li, WU Wei-Na, WANG Yuan

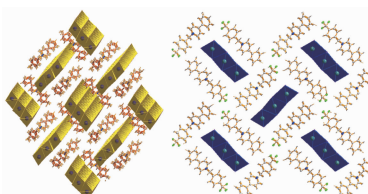


Two complexes $[\text{Cu}(\text{HL})\text{Cl}_2] \cdot \text{H}_2\text{O}$ and $[\text{ZnL}_2]$ have been synthesized and characterized. The $\text{Zn}^{(\text{II})}$ complex exhibits a different band from that of the ligand in the fluorescence emission spectra, probably due to the energy transferring from the ligand to the $\text{Zn}^{(\text{II})}$ ion.

DOI:10.11862/CJIC.2017.214
Chinese J. Inorg. Chem., 2017, 33:1849-1854

Syntheses and Crystal Structures of Two Homogeneous Organic-Inorganic Compounds Based on PbI_2 (English)

YUAN Guo-Jun, LIU Guang-Xiang, SHI Chao, SHAO Dong-Sheng

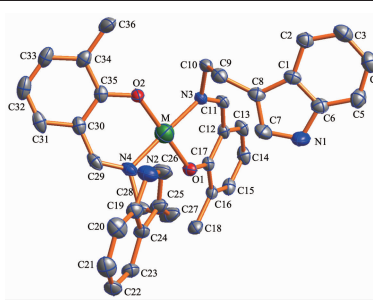


Iodoplumbate ion exhibits octahedron topology in compounds **1** and **2**, and all these octahedron topologies form 1D $[\text{Pb}_3\text{I}_6]_n$ polymeric chain through edge-sharing connecting modes.

DOI:10.11862/CJIC.2017.225
Chinese J. Inorg. Chem., 2017, 33:1855-1860

Two Mononuclear Ni(II) and Cu(II) Complexes Containing a Bidentate Schiff Base Ligand: Syntheses, Structures and Antibacterial Activities (English)

LIU Chao, LI Sha-Sha, YANG Min, BI Rong, YU Qing-Quan, ZHANG Li



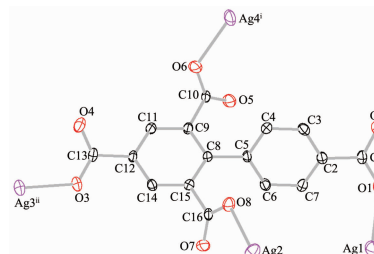
Two complexes, $\text{Ni}(\text{L})_2$ (**1**) and $\text{Cu}(\text{L})_2$ (**2**) based on HL ($\text{HL}=\text{N}-(3\text{-methylsalicylidene})\text{tryptamine}$) have been synthesized and investigated for their preliminary antibacterial activities. The results demonstrate that complexes **1** and **2** display more excellent inhibiting effects than the ligand.

DOI:10.11862/CJIC.2017.220
Chinese J. Inorg. Chem., 2017, 33:1861-1868

Syntheses, Structures, DNA Interaction of Ag(I) and Cd(II) Coordination Polymers Based on Biphenyl-2,4,4',6-tetracarboxylic Acid and Imidazo-phenanthrolin-phenoxo Acetic Acid (English)

LU Ya, LÜ Tian-Xi, HU Wei-Ji,
WU Xiao-Yong, ZHAO Guo-Liang

DOI:10.11862/CJIC.2017.215
Chinese J. Inorg. Chem., **2017**,**33**:1869-1875

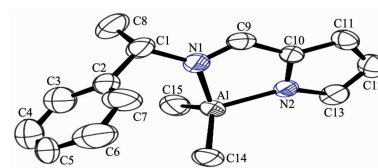


Two novel coordination polymers $[Ag_4(BPTC)]_n$ (**1**) and $[Cd(PIMPHC)_2]_n$ (**2**) were synthesized under hydrothermal reactions by using biphenyl-2,4,4',6-tetracarboxylic acid (H_4BPTC , $C_{16}H_{10}O_8$) and 2-(4-(1*H*-imidazo-2-[4,5-*f*] [1,10]phenanthrolinyl)phenoxy) acetic acid (HPIMPHC, $C_{21}H_{14}N_4O_3$).

Synthesis, Structure and Application in *rac*-Lactide Polymerization of Compound $[C_4H_3N\{CH=NCH(Me)C_6H_5\}-2]AlMe_2$ (English)

JIA Bin, HAO Jun-Sheng, TONG Hong-Bo,
WEI Xue-Hong, ZHOU Mei-Su,
LIU Dian-Sheng

DOI:10.11862/CJIC.2017.221
Chinese J. Inorg. Chem., **2017**,**33**:1876-1880

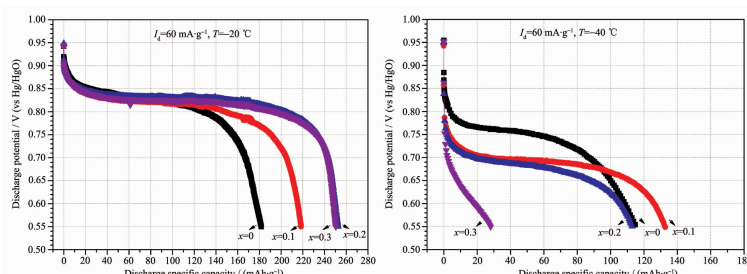


The reaction of Schiff base ligand (*d,l*)-*N*-(2-pyrrolylmethylene)-1-phenylethylamine with equivalent trimethylaluminum produced novel four-coordinated organoaluminum compound $[C_4H_3N\{CH=NCH(Me)C_6H_5\}-2]AlMe_2$. It is an active initiator for the polymerization of *rac*-lactide yielding the isotactic-rich polylactides.

Effects of Al Content on Low-Temperature and High-Rate Performance of $MmNi_{4.0-x}Co_{0.7}Mn_{0.3}Al_x$ Alloys (English)

TANG Zheng-Yao, ZHOU Wan-Hai,
ZHU Ding, WU Chao-Ling, HUANG Li-Wu,
LIU Kun, CHEN Yun-Gui

DOI:10.11862/CJIC.2017.228
Chinese J. Inorg. Chem., **2017**,**33**:1881-1888

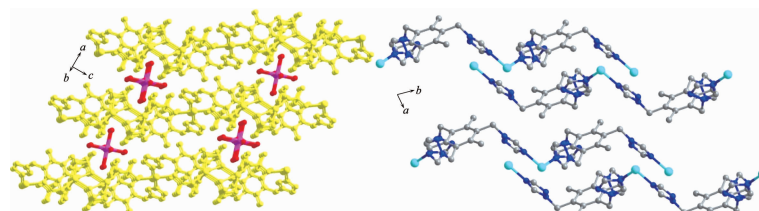


The discharge capacity still increases with the increase of Al content at $-20\text{ }^\circ\text{C}$, but gradually deteriorates when the temperature drops down to $-40\text{ }^\circ\text{C}$.

Syntheses, Crystal Structures and Fluorescence of Cadmium(II) and Zinc(II) Complexes Based on Flexible Tripodal Ligands (English)

WU Qi, SU Zhi, WANG Hong-Yan,
DONG Yi-Li, HU Jiong-Sheng, LIU Dong-Ju,
WU Chang, XU Yun, YING Ao, FANG Min,
LIU Hong-Ke

DOI:10.11862/CJIC.2017.196
Chinese J. Inorg. Chem., **2017**,**33**:1889-1895



Flexible tripodal nitrogen-containing ligands have been utilized to synthesize two 2D coordination polymers, which validate the strong coordination ability of imidazole- and triazolate-containing ligands.